Journal of Insights in Basic and Applied Sciences
مجلة رؤى في العلوم الأساسية والتطبيقية
Volume 1, Issue 2, 2025, Pages: 75-88
Journal homepage: https://jibas.com.ly/index.php/jibas/en

Stability and Local Bifurcation Analysis of a Measles *SVIR* Model with Waning Vaccine-Induced Immunity

Faisal O. Alqatrouni [1 *], Abdassalam B. H. Aldaikh [2]
[1,2] Department of Mathematics, Faculty of Science, University of Omar Al-Mukhtar, El-Beida, Libya

تحليل الاستقرار والتشعب المحلي لنموذج *SVIR* لمرض الحصبة مع تلاشي المناعة الناتجة عن اللقاح

فيصل عمر القطروني [1*]، عبد السلام بوحويش حمد الدايخ [2]
[2, 1] قسم الرياضيات، كلية العلوم، جامعة عمر المختار، البيضاء-ليبيا

*Corresponding author: faisalalqatrouni@gmail.ly

Received: October 14, 2025	Accepted: December 14, 2025	Published: December 25, 2025

Abstract:
This study presents a mathematical model to investigate the transmission dynamics of measles in a population following the introduction of vaccination. The population is divided into four epidemiological compartments: Susceptible (S), Vaccinated (V), Infected (I), and Recovered (R). A key feature of the model is the inclusion of waning immunity induced by vaccination over time. A thorough mathematical analysis is performed to establish the positivity and boundedness of the model solutions, along with the existence and local stability of equilibrium points. Furthermore, the model is analyzed for the occurrence of local bifurcations, including Hopf bifurcations, to identify potential complex dynamical behaviors. Numerical simulations are conducted to validate the analytical findings and assess the influence of key parameters on the system dynamics.

Keywords: Local Bifurcation, Measles, Stability, Vaccination.

الملخص
تقدم هذه الدراسة نموذجًا رياضيًا لدراسة ديناميكيات انتقال مرض الحصبة في مجتمعٍ ما بعد إدخال التطعيم. يُقسَّم السكان إلى أربع فئات وبائية: القابلون للإصابة (S)، والمطعَّمون (V)، والمصابون (I)، والمتعافون (R) . وتتمثل إحدى السمات الأساسية للنموذج في تضمين تلاشي المناعة الناتجة عن التطعيم بمرور الزمن.
يُجرى تحليل رياضي شامل لإثبات إيجابية وحدودية حلول النموذج، إلى جانب دراسة وجود نقاط التوازن واستقرارها المحلي. علاوة على ذلك، يُحلَّل النموذج لدراسة حدوث التشعبات المحلية، بما في ذلك تشعبات هوبف، بهدف تحديد السلوكيات الديناميكية المعقدة المحتملة. كما تُجرى محاكاة عددية للتحقق من النتائج التحليلية وتقييم تأثير المعلمات الرئيسية على ديناميكيات النظام.

الكلمات المفتاحية: التشعب المحلي، الحصبة، الاستقرار، التطعيم.

Introduction

Measles is a highly contagious viral disease with historical descriptions dating back to the 9th century, and the first detailed clinical account distinguishing it from other diseases was provided by Persian physician al-Razi in the 10th century. The causative virus was later isolated in the 20th century and the first licensed vaccine became

available in 1963 [1]. the world experienced millions of cases and hundreds of thousands of deaths every year. The measles vaccine is considered one of the most effective vaccines, leading to a significant decrease in cases and deaths associated with the disease. There are two doses of the measles vaccine; the first dose should be given at 12-15 months of age, while the second dose is usually administered at 4-6 years of age [2]. However, some recent studies [3], [4] have indicated a potential decline in the vaccine's effectiveness over time. These studies revealed that two doses of the vaccine may not provide lifelong immunity as previously believed, and that protection may diminish slightly each year. This decline in immunity could explain the increase in measles cases despite receiving vaccinations in childhood.

Mathematical models are of great importance in analyzing and understanding the dynamics of infectious diseases and epidemic spread, developing control policies, and formulating strategies to contain them. Interest in this field began with the famous SIR model introduced by Kermark and Mckendrick in 1927 [5]. This model established the first mathematical framework for studying and describing diseases transmitted through direct contact or interaction. Since then, scientific research and studies have advanced, and researchers have expanded this basic simple model to include various factors such as vaccination, treatment stages, immunity, and individual behavior within the community. For instance, researchers Kribs-Zaleta and Velasco-Hernandez presented in 2000 [6] an SIS type model incorporating the effect of development, Arino et al. [7], modified the traditional model to allow recovered individuals to enter a temporary immunity class instead of returning directly to the susceptible class, reflecting the nature of certain diseases that require clarification of this stage. Other studies focused on evaluating the effectiveness and impact of vaccination in reducing diseases. For instance, the study by Kribs-Zaleta and Martcheva [8] addressed the effect of vaccines in curbing the spread of diseases like Hepatitis (A, B). Meanwhile, SVIR models, as in the research of Alexander et al. [9] and Shim [10], focused on the spread dynamics of influenza in the presence of vaccines. On the other hand, studies such as d'Onofrio et al. [11] presented models to analyze and understand the impact of an individual's behaviors and decisions regarding vaccination on disease spread.

Bifurcation theory is an important branch of mathematics that specializes in studying qualitative or topological changes that occur or emerge in the structure of mathematical systems, such as the transformation of integral curves of vector fields or solutions of various differential equations. The importance and application of this theory lie primarily in the study and analysis of dynamical systems, where bifurcation occurs when a slight modification or change in parameter values (bifurcation parameters) leads to a radical change in the qualitative or topological behavior of the system, as illustrated in [12], [13], [14]. Bifurcation occurs in both continuous dynamical systems (represented by ordinary differential equations ODEs, delay differential equations DDEs, or partial differential equations PDEs; for example, see [15], [16], [17], [18], [19] and discrete dynamical systems (represented by maps; see, for example, [19], [20], [21], [22], [23], [24]. The term "bifurcation" was first introduced in 1885 by Henri Poincaré [27] in seminal mathematical research addressing this phenomenon. He named and classified different types of fixed points and described their characteristics. Perko L. [25] established the fundamental conditions for the occurrence of local bifurcation (such as saddle-node bifurcation, transcritical bifurcation, and pitchfork bifurcation). As for Hopf bifurcation, the necessary condition for its occurrence was formulated by Hirsch and Smale S. [26], while Haque M. and Venturino E**.** [27] explained the sufficient condition for the occurrence of this type of bifurcation. see, for example, [28], [29], [30]. In the same context, previous research efforts include studies by K. Qahtan Khalf et al. [31], and R. Kamel Naji and A. Ali Muhseen [32] on local bifurcation patterns and Hopf bifurcation around equilibrium points.

This study presents an SVIR-type mathematical model describing the spread dynamics of measles in the population. While our model uses a similar approach to many studies on measles transmission, it incorporates an analysis of vaccination impact by including critical factors such as full and partial vaccine efficacy, as well as waning immunity over time. Our research focuses on identifying the conditions that lead to the occurrence of Local bifurcations and Hopf bifurcations around certain equilibrium points of the proposed model.

Model description and formulation:

In this part, the model description is represented by a set of deterministic differential equations that illustrate the dynamics of infection transmission within the population concerning time (t). According to these equations, the population is divided into four categories:

Susceptible individuals $S(t)$ those who are at risk of infection but have not yet contracted it, Vaccinated individuals $V(t)$ those who have received the vaccine against the disease, Infected individuals $I(t)$ those who have contracted the infection and can transmit it to others, Recovered individuals $R(t)$ those who have been infected and have recovered from the disease.

The total population of these four categories is given by $N(t)$, which is the sum of the individuals in all categories.

The susceptible category $S(t)$ increases due to births at rate π, where a portion of newborns are unvaccinated. The decrease in this category is due to infection at rate $\frac{\beta SI}{N}$, vaccination at rate αS, and natural death at rate μS. Additionally, the category increases again due to waning vaccine efficacy over time at rate ωV.

The number of individuals in the vaccinated category $V(t)$ increases due to vaccination of the susceptible category at rate αS, individuals in this category can still be infected, but at a reduced rate $\frac{\beta VI(1-\varepsilon)}{N}$ due to vaccine efficacy. The decrease in this category is due to natural death at rate μV and waning immunity over time at rate ωV.

As for the infected category $I(t)$, the increase occurs either due to births or infection transmission from the susceptible category at rate $\frac{\beta SI}{N}$. Vaccinated individuals can also become infected but at a reduced rate $\frac{\beta VI(1-\varepsilon)}{N}$. The decrease in the infected category is due to recovery at rate δI, natural death μI, and disease-induced death at rate $\mu_I I$.

Finally, the last category, recovered individuals $R(t)$, increases due to the recovery of infected individuals at rate δI, and decreases solely due to natural death at rate μR. Therefore, the dynamics of the aforementioned set of differential equations describing the system can be mathematically represented as follows:

$$\left.\begin{aligned} \frac{dS}{dt} &= \pi - \frac{\beta SI}{N} - (\mu + \alpha)S + \omega V, \\ \frac{dV}{dt} &= \alpha S - \frac{\beta VI(1-\varepsilon)}{N} - \mu V - \omega V, \\ \frac{dI}{dt} &= \frac{\beta SI}{N} + \frac{\beta VI(1-\varepsilon)}{N} - (\delta I + \mu + \mu_I)I, \\ \frac{dR}{dt} &= \delta I - \mu R. \end{aligned}\right\} \quad (1)$$

The variables and parameters of the model are summarized in the following table.

Table 1. Variables and Parameters for Measles Dynamics

Variables and Parameters	Definition
$\boldsymbol{S}$	Susceptible individuals.
$\boldsymbol{V}$	Vaccinated individuals.
$\boldsymbol{I}$	Infected individuals.
$\boldsymbol{R}$	Recovered individuals.
$\boldsymbol{N}$	Total population.
$\boldsymbol{\pi}$	The birth rate
$\boldsymbol{\beta}$	The transmission rate of infection from susceptible individuals to infected individuals.
$\boldsymbol{\mu}$	The natural death rate.
$\boldsymbol{\mu_I}$	The mortality rate due to the disease.
$\boldsymbol{\alpha}$	The vaccination rate (the percentage of susceptible individuals who are vaccinated).
$\boldsymbol{\delta}$	The recovery rate from the disease.
$\boldsymbol{\varepsilon}$	Vaccine efficacy: $\mathbf{0} \leq \boldsymbol{\varepsilon} \leq \mathbf{1}$ (the percentage of protection provided by the vaccine).
$\boldsymbol{\omega}$	The rate of loss of immunity among vaccinated individuals (the return of vaccinated individuals to the susceptible category).

Accordingly, the progression of the disease described in system (1) is represented through the flow diagram provided in Figure 1.

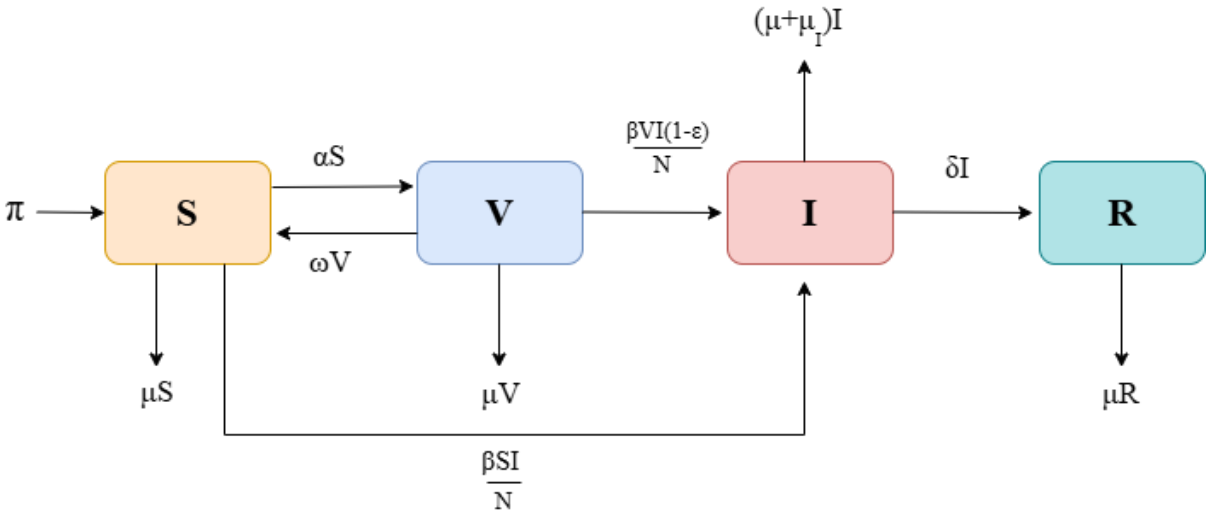

Figure 1. Flow diagram of system (1).

The Invariant Region

The SVIR model is widely used to describe measles transmission dynamics in human populations; it is natural to consider that all parameters and variables remain non-negative for $t \geq 0$. In what follows, we show that the model preserves the non-negativity of all model variables, provided that the initial conditions are non-negative.

Theorem 1. The feasible region (solution) of the measles model is defined as:

$$\Omega = \{(S, V, I, R) \in \mathbf{R}_+^4 : S(t) + V(t) + I(t) + R(t) = N(t) \leq \frac{\pi}{\mu}\} \qquad (2)$$

It is positively invariant and attracting.

Proof: considering the total population as $N(t) = S(t) + V(t) + I(t) + R(t)$, and under the assumption of non-negative initial conditions $(S(0), V(0), I(0), R(0))$, the sum of the system equations gives the evolution of the total population over time, i.e.

$$\frac{dN}{dt} = \frac{dS}{dt} + \frac{dV}{dt} + \frac{dI}{dt} + \frac{dR}{dt}$$

That is

$$\frac{dN}{dt} = \pi - \mu N$$

Solving the first-order linear differential equation:

$$\frac{dN}{dt} + \mu N = \pi$$

Which has the solution

$$N(t) = N(0)e^{-\mu t} + \frac{\pi}{\mu}(1 - e^{-\mu t})$$

$$N(t) \leq \frac{\pi}{\mu}$$

The relation $N(t) \leq \frac{\pi}{\mu}$ remains satisfied provided that $N(0) \leq \frac{\pi}{\mu}$ holds, which makes the region Ω a positively invariant set for the system trajectories. If $N(0)$ exceeds this threshold, i.e., $N(0) > \frac{\pi}{\mu}$, then one of two scenarios will occur: either the solution reaches region Ω within a finite time, or the total population tends toward the value

$\frac{\pi}{\mu}$ while the infected compartments shrink to zero. It follows that region Ω possesses an attracting property, ensuring that all solutions emanating from domain $\mathbf{R}_+^4$ will eventually settle within this region Ω. Accordingly, the analysis of the dynamic measles patient model can be confined to the domain Ω, which both mathematically and epidemiologically is properly and rigorously formulated, thus guaranteeing its practical validity. Therefore, Ω is positively invariant and all attract solutions in $\mathbf{R}_+^4$.

Positivity of the solution of the system (1)

Theorem 2. The solution set {S(t), V(t), I(t), R(t)} of the system (1) with positive initial values in Ω. remains positive in Ω for all time $t > 0$.

Proof: The following can be obtained from the first equation of the system (1):

$$\frac{dS}{dt} = \pi - \frac{\beta SI}{N} - (\mu + \alpha)S + \omega V$$

We can obtain that

$$\frac{dS}{dt} \geq -\left(\frac{\beta I}{N} + \mu + \alpha\right)S$$

By separation of variables, $S \neq 0$

$$\frac{dS}{S(t)} \geq -\left(\frac{\beta I}{N} + \mu + \alpha\right)dt$$

Which gives

$$S(t) \geq S(0)e^{-\left(\frac{\beta I}{N}+\mu+\alpha\right)t} \geq 0$$

Then,

$$S(t) \geq 0 \text{ for all } t \geq 0.$$

The remaining variables can be determined by following the same steps, which confirms that all variables have positive values.

Existence of equilibrium points of the system (1)

The existence of all potential equilibrium points in the system (1) is studied in this part. Since the recovered class *R* depends only on the infected class *I*, the fourth equation of system (1) can be explicitly solved for R once the value of *I* is known. The R value asymptotically goes to zero if $I = 0$; conversely, R tends toward the following value if $I = I_c$, where I_c is a constant greater than zero:

$$R = (3\frac{\delta I_C}{\mu} \qquad (3)$$

Accordingly, the equations listed below are the first three equations of system (1) that will be the focus of the analysis. Once these equations are examined, thus, equation (3) can help to determine the value of *R*.

$$\left.\begin{aligned} \frac{dS}{dt} &= \pi - \frac{\beta SI}{N} - (\mu + \alpha)S + \omega V \\ \frac{dV}{dt} &= \alpha S - \frac{\beta VI(1-\varepsilon)}{N} - \mu V - \omega V \\ \frac{dI}{dt} &= \frac{\beta SI}{N} + \frac{\beta VI(1-\varepsilon)}{N} - (\delta + \mu + \mu_I)I \end{aligned}\right\} \qquad (4)$$

There is an equilibrium point in system (4) known as the disease-free equilibrium point (DFE) when $I = 0$, which is represented by $E^0 = (S^0, V^0, 0)$ where:

$$\left.\begin{aligned} S^0 &= \frac{\pi(\mu+\omega)}{\mu(\mu+\alpha)+\omega\mu} \\ V^0 &= \frac{\alpha\pi}{\mu(\mu+\alpha)+\omega\mu} \end{aligned}\right\} \qquad (5)$$

Conversely, $E^* = (S^*, V^*, I^*)$ represents the endemic equilibrium point (EE) of system (4) if $I \neq 0$, where S^*,V^*, and I^* are identified as the positive solutions to the following equations:

$$\begin{aligned}
&\pi - \frac{\beta SI}{N} - (\mu + \alpha)S + \omega V = 0 \\
&\alpha S - \frac{\beta VI(1-\varepsilon)}{N} - \mu V - \omega V = 0 \\
&\frac{\beta SI}{N} + \frac{\beta VI(1-\varepsilon)}{N} - (\delta + \mu + \mu_I)I = 0
\end{aligned} \qquad (6)$$

Solving these equations analytically gives

$$\left.\begin{aligned}
S^* &= \frac{\pi[\beta I(1-\varepsilon)+(\mu+\omega)N]}{\beta^2 I^{*2}(1-\varepsilon)+\beta I^* N[(\mu+\omega)+(1-\varepsilon)[\mu+\alpha]]+\mu N^2(\mu+\alpha+\omega)} \\
V^* &= \frac{\alpha\pi N^2}{\beta^2 I^{*2}(1-\varepsilon)+\beta I^* N[(\mu+\omega)+(1-\varepsilon)[\mu+\alpha]]+\mu N^2(\mu+\alpha+\omega)}
\end{aligned}\right\} \qquad (7)$$

Substituting the expressions given in (7) into system (6) yields a cubic polynomial equation in terms of the endemic infected population I^*, given by:

$$I^* = D_1 I^3 + D_2 I^2 + D_3 I \qquad (8)$$

Equation (8) is a third-degree polynomial in I^*, where the coefficients D_1, D_2 and D_3 depend on the model parameters as defined below:

$$\begin{aligned}
D_1 &= -N\beta^2(1-\varepsilon)(\delta+\mu+\mu_I) < 0 \\
D_2 &= (N\beta(\beta\pi(1-\varepsilon) - N(\delta+\mu+\mu_I)[(\mu+\omega)+(1-\varepsilon)(\mu+\alpha)])) \\
D_3 &= N^2\left(\beta\big(\pi(\mu+\omega)+\alpha\pi(1-\varepsilon)\big) - N\mu(\mu+\omega+\alpha)(\delta+\mu+\mu_I)\right)
\end{aligned}$$

The presence of a unique positive solution I^* to equation (8) can be established via Descartes rule of signs, provided that at least one of the following conditions holds.

$$\beta\pi(1-\varepsilon) < N(\delta+\mu+\mu_I)[(\mu+\omega)+(1-\varepsilon)(\mu+\alpha)] \qquad (9.a)$$

$$\beta\big(\pi(\mu+\omega)+\alpha\pi(1-\varepsilon)\big) > N\mu(\mu+\omega+\alpha)(\delta+\mu+\mu_I) \qquad (9.b)$$

Local stability analysis

In this part, system (4) is analyzed for local stability at E^0 and E^*, as established in the theorems that follow.

Theorem 3. For system (4), the disease-free equilibrium point $\mathrm{E}^0 = (\mathrm{S}^0, \mathrm{V}^0, 0)$ is locally asymptotically stable provided that the condition below is satisfied:

$$\frac{\beta(\mathrm{S}^0+\mathrm{V}^0(1-\varepsilon))}{N(\delta+\mu+\mu_I)} < 1 \qquad (10.a)$$

and qualifies as a saddle-point if:

$$\frac{\beta(S^0+V^0(1-\varepsilon))}{N(\delta+\mu+\mu_I)} > 1 \qquad (10.b)$$

Proof: The Jacobian matrix corresponding to system (4) is given by:

$$J = \begin{bmatrix}
-\frac{\beta I}{N} - (\mu+\alpha) & \omega & -\frac{\beta S}{N} \\
\alpha & -\frac{\beta I(1-\varepsilon)}{N} - (\mu+\omega) & -\frac{\beta V(1-\varepsilon)}{N} \\
\frac{\beta I}{N} & \frac{\beta I(1-\varepsilon)}{N} & \frac{\beta(S+V(1-\varepsilon))}{N} - (\delta+\mu+\mu_I)
\end{bmatrix}$$

and hence

$$J(\mathrm{E}^0) = \begin{bmatrix} -(\mu+\alpha) & \omega & -\frac{\beta S^0}{N} \\ \alpha & -(\mu+\omega) & -\frac{\beta V^0(1-\varepsilon)}{N} \\ 0 & 0 & \frac{\beta(S^0+V^0(1-\varepsilon))}{N} - (\delta+\mu+\mu_I) \end{bmatrix}$$

$$|J(\mathrm{E}^0) - \lambda| = \begin{vmatrix} -(\mu+\alpha)-\lambda & \omega & -\frac{\beta S^0}{N} \\ \alpha & -(\mu+\omega)-\lambda & -\frac{\beta V^0(1-\varepsilon)}{N} \\ 0 & 0 & \frac{\beta(S^0+V^0(1-\varepsilon))}{N} - (\delta+\mu+\mu_I) - \lambda \end{vmatrix} = 0$$

$$\left(\frac{\beta(S^0+V^0(1-\varepsilon))}{N} - (\delta+\mu+\mu_I) - \lambda\right) \begin{vmatrix} -(\mu+\alpha)-\lambda & \omega \\ \alpha & -(\mu+\omega)-\lambda \end{vmatrix} = 0$$

The Jacobian matrix $J(\mathrm{E}^0)$ has the following characteristic equation:

$$\left(\frac{\beta(S^0+V^0(1-\varepsilon))}{N} - (\delta+\mu+\mu_I) - \lambda\right)[\lambda^2 + A\lambda + B] = 0 \qquad (11)$$

where:

$$\left.\begin{aligned} A &= [(\mu+\alpha)+(\mu+\omega)] > 0 \\ B &= [\mu(\mu+\omega+\alpha)] > 0 \end{aligned}\right\} \qquad (12.a)$$

Consequently, equation (9) has the following roots (eigenvalues) of $J(\mathrm{E}^0)$:

$$\lambda_{S,V} = \frac{-A}{2} \pm \frac{(\alpha+\omega)}{2} < 0 \qquad (12.b)$$

$$\lambda_I = \left(\frac{\beta(S^0+V^0(1-\varepsilon))}{N} - (\delta+\mu+\mu_I)\right) \qquad (12.c)$$

where the eigenvalues λ_S, λ_V, and λ_I represent the system dynamics behavior in the direction of the variables *S*, *V*, and *I*, respectively.

Both λ_S and λ_V are not positive. In contrast, λ_I, the third eigenvalue, may be negative or positive depending on whether conditions (10.a) and (10.b) are satisfied, respectively.

As a result, E^0 remains asymptotically stable when condition (10.a) is satisfied, but it becomes a saddle point if condition (10.b) is satisfied; therefore, the proof is finished.

Theorem 4. For system (4), local asymptotic stability is ensured if the endemic equilibrium point $E^* = (S^*, V^*, I^*)$ exists and the following conditions hold:

$$\frac{\beta(S^0+V^0(1-\varepsilon))}{N} < (\delta+\mu+\mu_I) \qquad (13.a)$$

and

$$\beta\left[S^*\left(2\omega+3\alpha(1-\varepsilon)\right) + \mathrm{V}^*(\varepsilon-1)\left(3\omega+2\alpha(1-\varepsilon)\right)\right] < 2\left(\omega+\alpha(1-\varepsilon)\right)(\delta+\mu+\mu_I) \qquad (13.b)$$

Proof: By computing the Jacobian matrix of system (4) at the E^*:

$$J(E^*) = \begin{bmatrix} -\frac{\beta I^*}{N} - (\mu + \alpha) & \omega & -\frac{\beta S^*}{N} \\ \alpha & -\frac{\beta I^*(1-\varepsilon)}{N} - (\mu + \omega) & \frac{-\beta V^*(1-\varepsilon)}{N} \\ \frac{\beta I^*}{N} & \frac{\beta I^*(1-\varepsilon)}{N} & \frac{\beta(S^* + V^*(1-\varepsilon))}{N} - (\delta + \mu + \mu_I) \end{bmatrix}$$

Therefore, this is the characteristic equation for system (4) at the endemic equilibrium:

$$\lambda^3 + A_1\lambda^2 + A_2\lambda + A_3 = 0$$

Here:

$A_1 = -[a_{11} + a_{22} + a_{33}]$.

$A_2 = a_{11}a_{22} - a_{12}a_{21} + a_{11}a_{33} - a_{13}a_{31} + a_{22}a_{33} - a_{23}a_{32}$.

$A_3 = -[a_{11}a_{22}a_{33} + a_{12}a_{23}a_{31} + a_{13}a_{21}a_{32} - a_{13}a_{22}a_{31} - a_{11}a_{23}a_{32} - a_{12}a_{21}a_{33}]$.

$= -[a_{33}(a_{11}a_{22} - a_{12}a_{21}) + a_{12}a_{23}a_{31} + a_{13}a_{21}a_{32} - a_{13}a_{22}a_{31} - a_{11}a_{23}a_{32}]$.

Further:

$\Delta = A_1A_2 - A_3$

$= -(a_{11} + a_{22})(a_{11}a_{22} - a_{12}a_{21})$

$-(a_{11} + a_{33})(a_{11}a_{33} - a_{13}a_{31})$

$-(a_{22} + a_{33})(a_{22}a_{33} - a_{23}a_{32})$

$-2a_{11}a_{22}a_{33} + a_{12}a_{23}a_{31} + a_{13}a_{21}a_{32}$

Due to the *Routh-Hurwitz* criterion, if $A_1 > 0, A_3 > 0$, and $\Delta = A_1A_2 - A_3 > 0$, then the endemic equilibrium point E^* will be locally asymptotically stable.

It is obvious that if condition (13.a) is true, $A_1 > 0$ and $A_3 > 0$. Provided that conditions (13) (a-b) are satisfied. Then $\Delta = A_1A_2 - A_3 > 0$. This completes the proof.

The local bifurcation analysis of the system (4)

This part investigates the presence of local bifurcations, namely, saddle-node, transcritical, and pitchfork types for system (4) around the equilibrium point, using the Sotomayor criterion [25]. The Jacobian matrix at (E^0, δ_0) for system (4) can be expressed as follows:

$$J = Df(E^0, \delta_0)$$

where:

$$\delta_0 = \frac{\beta(S^0 + V^0(1-\varepsilon))}{N} - (\mu + \mu_I) \qquad (14)$$

$$J = Df(E^0, \delta_0) = \begin{bmatrix} -(\mu + \alpha) & \omega & -\frac{\beta S^0}{N} \\ \alpha & -(\mu + \omega) & -\frac{\beta V^0(1-\varepsilon)}{N} \\ 0 & 0 & 0 \end{bmatrix}$$

The third eigenvalue λ_I, is equal to zero ($\lambda_I = 0$), but λ_S and $\lambda_{V,}$ as provided in equation (12.b), are negative. Furthermore, $K = (k_1, k_2, k_3)^T$ is the eigenvector that corresponds to λ_I satisfying the next condition:

$$JK = \lambda K \text{ then } JK = 0$$

Therefore

$$\begin{bmatrix} -(\mu+\alpha) & \omega & -\frac{\beta S^0}{N} \\ \alpha & -(\mu+\omega) & -\frac{\beta V^0(1-\varepsilon)}{N} \\ 0 & 0 & 0 \end{bmatrix} \cdot \begin{bmatrix} k_1 \\ k_2 \\ k_3 \end{bmatrix} = 0$$

From this, we get that:

$$-(\mu+\alpha)k_1 + \omega k_2 - \frac{\beta S^0}{N} k_3 = 0 \quad (15.a)$$

$$\alpha k_1 - (\mu+\omega)k_2 - \frac{\beta V^0(1-\varepsilon)}{N} k_3 = 0 \quad (15.b)$$

Solving the aforementioned system of equations gives:

$$k_1 = hk_3 \; ; k_2 = gk_3$$

where

$$h = \frac{-\beta\left[V^0\omega(1-\varepsilon)(\mu+\alpha)^2 + \left(S^0(\mu^3+\mu^2(\omega+2\alpha)+\alpha\omega(2\mu+\alpha)+\alpha^2\mu)\right)\right]}{N[\mu(\mu+\omega+\alpha)]},$$

and

$$g = \frac{\beta[\alpha S^0 + V^0(1-\varepsilon)(\mu+\alpha)]}{N[\mu(\mu+\omega+\alpha)]}.$$

Here k_3 can be any real value that is not zero.

Therefore

$$K = \begin{bmatrix} hk_1 \\ gk_2 \\ k_3 \end{bmatrix}$$

Furthermore, the eigenvector $W = (w_1, w_2, w_3)^T$ corresponding to λ_I of J^T can be written as:

$$\begin{bmatrix} -(\mu+\alpha) & \alpha & 0 \\ \omega & -(\mu+\omega) & 0 \\ -\frac{\beta S^0}{N} & -\frac{\beta V^0(1-\varepsilon)}{N} & 0 \end{bmatrix} \cdot \begin{bmatrix} w_1 \\ w_2 \\ w_3 \end{bmatrix} = 0$$

Hence, we have:

$$w = \begin{bmatrix} 0 \\ 0 \\ w_3 \end{bmatrix}$$

Let w_3 be any nonzero real number. System (4) is then expressed in the vector form as follows:

$$\frac{dX}{dt} = f(x)$$

where $X = (S, V, I)^T$ and $f = (f_1, f_2, f_3)$ with $f_i, i = 1,2,3$ as presented in system (4), thus, by determining $\frac{df}{d\delta} = f_\delta$, we obtain that:

$$f_\delta = \begin{bmatrix} 0 & 0 & 0 \\ 0 & 0 & 0 \\ 0 & 0 & -I \end{bmatrix} = \begin{bmatrix} 0 \\ 0 \\ -I \end{bmatrix}$$

Then

$$f_\delta(E^0, \delta_0) = \begin{bmatrix} 0 \\ 0 \\ 0 \end{bmatrix}$$

Therefore

$$W^T . f_\delta(E^0, \delta_0) = 0$$

Thus, based on the Sotomayor theorem**,** at δ_0 the system does not exhibit a Saddle-node bifurcation around E^0.

To analyze the possible emergence of different types of bifurcation, the Jacobian matrix Df_δ is evaluated at the disease-free equilibrium point (E^0, δ_0), with respect to the state variables in vector X.

$$Df_\delta(E^0, \delta_0) = \begin{bmatrix} 0 & 0 & 0 \\ 0 & 0 & 0 \\ 0 & 0 & -1 \end{bmatrix}$$

so

$$W^T . [Df_\delta(E^0, \delta_0) . K] = -k_3 w_3 \neq 0$$

Furthermore, based on Sotomayor's theorem, given that the following results are true, in addition to what has been previously established

$$W^T . [D^2 f(E^0, \delta_0) . (K, k)] \neq 0$$

In this case, $Df(E^0, \delta_0)$ represents the Jacobian matrix evaluated at E^0 and δ_0, as a result, system (4) exhibits a transcritical bifurcation, but a pitch-fork bifurcation is unlikely. given that it is known as:

$$[D^2 f(E^0, \delta_0) . (K, k)] = \begin{bmatrix} \frac{-2\beta h}{N} k_3^2 \\ \frac{-2\beta g(1-\varepsilon)}{N} k_3^2 \\ \frac{2\beta(h + g(1-\varepsilon))}{N} k_3^2 \end{bmatrix}$$

Therefore

$$W^T . [D^2 f(E^0, \delta_0) . (K, k)] = \frac{2\beta(h + g(1-\varepsilon))}{N} k_3^2 \neq 0$$

Hence, whenever the parameter δ crosses through the bifurcation value δ_0, system (4) exhibits a transcritical bifurcation in the neighborhood of E^0.

The Hopf-bifurcation analysis of system (4)

A Hopf-bifurcation occurring close to the endemic equilibrium point is investigated in this section. $A_i, i = 1,2,3$, are positive if condition (13.a) has been satisfied, according to the coefficients of the characteristic equation determined by a local stability analysis of system (4) around E^*. On the other hand, $\Delta = A_1 A_2 - A_3$ is positive if condition (13.b) has been satisfied, and therefore, according to the theorem of Hopf-bifurcation [27], a Hopf-bifurcation does not occur in this case. The absence of a Hopf bifurcation in this model carries significant epidemiological implications. It indicates that the measles transmission dynamics, under the studied parameters, do not exhibit sustained oscillations or recurrent epidemic waves. This means that once the system stabilizes—whether in a disease-free or endemic state—it tends to remain in that state without periodic unexpected fluctuations. Such dynamic stability facilitates long-term control strategy planning, as disease behavior becomes more predictable.

Numerical analysis

The current section aims to investigate the overall dynamic behavior of the system (1) through numerical simulations. The temporal evolution of all epidemiological compartments, namely the susceptible $S(t)$, vaccinated $V(t)$, infected $I(t)$, and recovered $R(t)$, is illustrated by solving the system over a finite time interval.is illustrated by solving the system over a finite time interval, In Figure 2, the trajectories are distinguished by color, where the susceptible population $S(t)$ is represented by the blue curve, the vaccinated population $V(t)$ by the green curve, the infected population $I(t)$ by the red curve, and the recovered population $R(t)$ by the black curve. For the simulations, the initial conditions were chosen as $S(0) = 990, V(0) = 0, I(0) = 10$, and $R(0) = 0$, representing a population with a small number of initial infections. The parameter values used in the numerical analysis are summarized in the following table.

Table 2. Parameter values used in the numerical analysis

Parameter	Value	Source
$\boldsymbol{\pi}$	10	Assumed
$\boldsymbol{\beta}$	0.3	Assumed
$\boldsymbol{\alpha}$	0.05	Assumed
$\boldsymbol{\delta}$	0.1	[4]
$\boldsymbol{\mu}$	0.01	Assumed
$\boldsymbol{\mu_I}$	0.02	Assumed
$\boldsymbol{\omega}$	0.02	[5,6]
$\boldsymbol{\varepsilon}$	[0,1]	control parameter

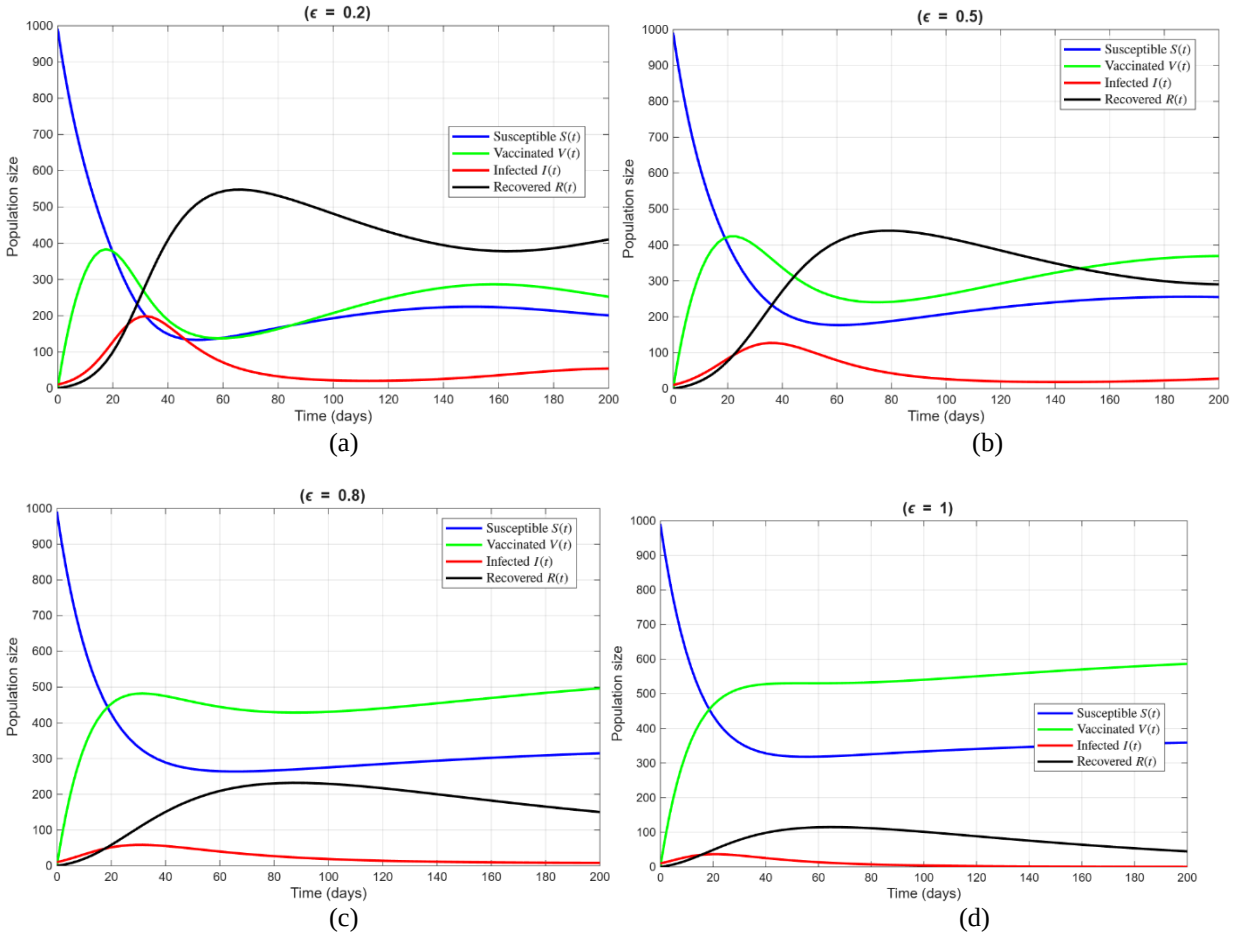

Figure 2. Time evolution of the SVIR compartments for different values of vaccine efficacy ε.

The results demonstrate that increasing vaccine efficacy significantly reduces the number of infected individuals over time. In particular, as ε approaches unity, the probability of infection among vaccinated individuals decreases, leading to a substantial decline in the infected population.

Results and discussion

The mathematical analysis conducted in this study provides important insights into the impact of vaccination on measles transmission dynamics. The presence of a transcritical bifurcation near the disease-free equilibrium indicates a critical threshold that governs the transition between disease elimination and persistence, highlighting the importance of maintaining high vaccination coverage and efficacy to ensure disease control. In contrast, no Hopf bifurcation was detected in the model, indicating the absence of sustained oscillations or recurrent epidemic waves at equilibrium points, which reflects the stability of the system under the current conditions. This means that any short-term fluctuations in infection numbers tend to dissipate quickly, making the long-term behavior of the disease more predictable. Furthermore, the absence of both saddle-node and pitchfork bifurcations supports the structural stability of the model under small perturbations. Epidemiologically, this implies that measles tends to stabilize either in a disease-free state or a relatively steady endemic state, unless critical parameters such as vaccine efficacy or coverage undergo substantial changes a consideration of particular importance given the phenomenon of waning immunity over time.

Numerical simulations confirmed these analytical results, showing that increased vaccine efficacy leads to a significant reduction in the number of infections, while decreased vaccine efficacy due to waning immunity increases the size of the susceptible population even in highly vaccinated communities. When vaccine efficacy approaches its maximum value, the probability of infection among vaccinated individuals decreases markedly, underscoring the crucial role of highly effective vaccines in controlling measles transmission.

From a public health perspective, these findings emphasize the need to design flexible vaccination policies that include booster programs to maintain immunity levels in the population over the long term, with a focus on sustaining high vaccination coverage and minimizing vaccine failure. Such measures ensure stability in disease dynamics and prevent potential outbreaks, even in communities experiencing gradual declines in immunity.

Conclusion

In this study, a mathematical model was developed and analyzed to describe the transmission dynamics of measles under the influence of vaccination. The existence and local stability of equilibrium points were rigorously examined. Bifurcation analysis revealed the occurrence of a transcritical bifurcation in the neighborhood of the disease-free equilibrium, while both saddle-node and pitchfork bifurcations were found to be absent. In addition, the analysis showed that no Hopf bifurcation occurs in the proposed model, indicating the absence of sustained oscillatory behavior near the equilibrium points. Numerical simulations supported the analytical findings and demonstrated that increasing vaccine efficacy significantly reduces the number of infected individuals over time. From an epidemiological perspective, these results highlight the critical role of vaccination-related parameters in determining long-term disease control.

Future work

Finally, future extensions of the proposed SVIR model may incorporate time delays to account for the latency period between infection and symptom onset, as well as the delay between vaccination and the acquisition of effective immunity. Such extensions could lead to richer dynamical behaviors, including possible oscillatory dynamics. Moreover, incorporating social and behavioral factors, such as vaccine hesitancy or heterogeneous contact patterns, would provide a more realistic framework for assessing measles transmission and designing effective control strategies.

References

[1] 'History of measles vaccination'. Accessed: Dec. 24, 2025. [Online]. Available: https://www.who.int/news-room/spotlight/history-of-vaccination/history-of-measles-vaccination

[2] S. Edward, 'A Mathematical Model for Control and Elimination of the Transmission Dynamics of Measles', *Appl. Comput. Math.*, vol. 4, no. 6, p. 396, 2015, doi: 10.11648/j.acm.20150406.12.

[3] J. Zibolenová *et al.*, 'Quantification of Waning Immunity After Measles Vaccination—Evidence From a Seroprevalence Study', *Am. J. Epidemiol.*, vol. 192, no. 8, pp. 1379–1385, Aug. 2023, doi: 10.1093/aje/kwad065.

[4] L. Yang, B. T. Grenfell, and M. J. Mina, 'Waning immunity and re-emergence of measles and mumps in the vaccine era', *Curr. Opin. Virol.*, vol. 40, pp. 48–54, Feb. 2020, doi: 10.1016/j.coviro.2020.05.009.

[5] W. O. Kermack and A. G. McKendrick, 'A contribution to the mathematical theory of epidemics', *Proc. R. Soc. Lond. Ser. Contain. Pap. Math. Phys. Character*, vol. 115, no. 772, pp. 700–721, Aug. 1927, doi: 10.1098/rspa.1927.0118.

[6] C. M. Kribs-Zaleta and J. X. Velasco-Hernández, 'A simple vaccination model with multiple endemic states', *Math. Biosci.*, vol. 164, no. 2, pp. 183–201, Apr. 2000, doi: 10.1016/S0025-5564(00)00003-1.

[7] C. C. McCluskey and P. V. D. Driessche, ‘Global Analysis of Two Tuberculosis Models’, *J. Dyn. Differ. Equ.*, vol. 16, no. 1, pp. 139–166, Jan. 2004, doi: 10.1023/B:JODY.0000041283.66784.3e.
[8] C. M. Kribs-Zaleta and M. Martcheva, ‘Vaccination strategies and backward bifurcation in an age-since-infection structured model’, *Math. Biosci.*, vol. 177–178, pp. 317–332, May 2002, doi: 10.1016/S0025-5564(01)00099-2.
[9] M. E. Alexander, C. Bowman, S. M. Moghadas, R. Summers, A. B. Gumel, and B. M. Sahai, ‘A Vaccination Model for Transmission Dynamics of Influenza’, *SIAM J. Appl. Dyn. Syst.*, vol. 3, no. 4, pp. 503–524, Jan. 2004, doi: 10.1137/030600370.
[10] E. Shim, ‘An epidemic model with immigration of infectives and vaccination’, 2009, doi: 10.14288/1.0080044.
[11] A. d’Onofrio, P. Manfredi, and E. Salinelli, ‘Vaccinating behaviour, information, and the dynamics of SIR vaccine preventable diseases’, *Theor. Popul. Biol.*, vol. 71, no. 3, pp. 301–317, May 2007, doi: 10.1016/j.tpb.2007.01.001.
[12] J. Guckenheimer and P. Holmes, *Nonlinear Oscillations, Dynamical Systems, and Bifurcations of Vector Fields*, vol. 42. in Applied Mathematical Sciences, vol. 42. New York, NY: Springer New York, 1983. doi: 10.1007/978-1-4612-1140-2.
[13] A. A. Andronov, A. G. Maier, I. I. Gordon, and E. A. Leontovich, *Theory Of Bifurcations Of Dynamic Systems On A Plane*. NASA Technical Translations, 1971. Accessed: July 29, 2025. [Online]. Available: http://archive.org/details/a.-a.-andronov-e.-a.-leontovich-i.-i.-gordon-and-a.-g.-maier-theory-of-bifurcati
[14] Y. Kuznetsov, *Elements of Applied Bifurcation Theory*. Springer Science & Business Media, 1998.
[15] P. Blanchard, R. L. Devaney, G. R. Hall, and B. Persaud, *Differential equations*, 4. ed., International ed. Independence, KY: Brooks/Cole, Cengage Learning, 2011.
[16] D. K. Arrowsmith and C. M. Place, *Ordinary Differential Equations: A Qualitative Approach with Applications*. Chapman and Hall, 1982.
[17] R. Hoyle, ‘Some ideas from dynamical systems’, presented at the Isaac Newton Institute seminar, Cambridge, UK, 2005. [Online]. Available: chrome-extension://efaidnbmnnnibpcajpcglclefindmkaj/https://www.newton.ac.uk/files/seminar/20050801113012301-149145.pdf
[18] N. A. M. Monk, ‘Oscillatory Expression of Hes1, p53, and NF-κB Driven by Transcriptional Time Delays’, *Curr. Biol.*, vol. 13, no. 16, pp. 1409–1413, Aug. 2003, doi: 10.1016/S0960-9822(03)00494-9.
[19] S. Wiggins, *Introduction to Applied Nonlinear Dynamical Systems and Chaos*, vol. 2. in Texts in Applied Mathematics, vol. 2. New York, NY: Springer New York, 1990. doi: 10.1007/978-1-4757-4067-7.
[20] R. L. Devaney, *An introduction to chaotic dynamical systems*, Second edition. Boca Raton London New York: CRC Press, 2018.
[21] C. H. Edwards and D. E. Penney, *Elementary differential equations*, 6. ed. Upper Saddle River, N.J: Pearson Prentice Hall, 2008.
[22] A. Verdugo and R. Rand, ‘Hopf bifurcation in a DDE model of gene expression’, *Commun. Nonlinear Sci. Numer. Simul.*, vol. 13, no. 2, pp. 235–242, Mar. 2008, doi: 10.1016/j.cnsns.2006.05.001.
[23] E. G. Wiens, ‘Egwald Mathematics — Nonlinear Dynamics: Bifurcations in Two Dimensional Flows’. Accessed: July 29, 2025. [Online]. Available: https://www.egwald.ca/nonlineardynamics/bifurcations.php
[24] W.-B. Zhang, *Discrete dynamical systems, bifurcations and chaos in economics*. in Mathematics in science and engineering, no. v. 204. Amsterdam Boston: Elsevier, 2006.
[25] L. Perko, *Differential Equations and Dynamical Systems*, vol. 7. in Texts in Applied Mathematics, vol. 7. New York, NY: Springer New York, 2001. doi: 10.1007/978-1-4613-0003-8.
[26] M. W. Hirsch, *Differential equations, dynamical systems, and linear algebra*. in Pure and applied mathematics, no. v. 60. New York: Academic Press, 1974.
[27] M. Haque and E. Venturino, ‘Increase of the prey may decrease the healthy predator population in presence of a disease in the predator’, 2006, Accessed: July 29, 2025. [Online]. Available: https://iris.unito.it/handle/2318/10329
[28] D. Greenhalgh, Q. J. A. Khan, and F. I. Lewis, ‘Hopf bifurcation in two SIRS density dependent epidemic models’, *Math. Comput. Model.*, vol. 39, no. 11–12, pp. 1261–1283, June 2004, doi: 10.1016/j.mcm.2004.06.007.
[29] B. D. Hassard, N. D. Kazarinoff, and Y.-H. Wan, *Theory and applications of Hopf bifurcation*. in London Mathematical Society lecture note series, no. 41. Cambridge ; New York: Cambridge University Press, 1981.
[30] H. W. Hethcote, L. Yi, and J. Zhujun, ‘Hopf bifurcation in models for pertussis epidemiology’, *Math. Comput. Model.*, vol. 30, no. 11–12, pp. 29–45, Dec. 1999, doi: 10.1016/S0895-7177(99)00196-X.
[31] K. Q. Khalaf, A. A. Majeed, and R. K. Naji, ‘The local bifurcation and the hopf bifurcation for eco-epidemiological system with one infectious disease’, *G. E. N.*, vol. 31, no. 1, pp. 18–41, 2015, Accessed: July 29, 2025. [Online]. Available: http://emis.muni.cz/journals/GMN/yahoo_site_admin/assets/docs/3_GMN-9262-V31N1.35975713.pdf

[32] R. Naji and A. Muhseen, ‘Stability and bifurcation of epidemic model’, *Iraqi J. Sci.*, vol. 54, no. Mathematics conf, pp. 764–774, 2013, Accessed: July 29, 2025. [Online]. Available: https://www.ijs.uobaghdad.edu.iq/index.php/eijs/article/view/12458
[33] Naji R, Muhseen A. Stability analysis with bifurcation of an SVIR epidemic model involving immigrants. Iraqi J Sci. 2013;54(2):397–408.